

Supplementary Information

Engineering of Redox-triggered Polymeric Lipid Hybrid Nanocarriers for Selective Drug Delivery to Cancer Cells

B. Siva Lokesh ^{a,c,#}, Suresh Ajmeera ^{a,d,e,#}, Rajat Choudhary ^{a,c}, Sanjaya Kumar Moharana ^{b,c},
C. S. Purohit ^{b,c}, V Badireenath Konkimalla ^{a,c,*}

^a School of Biological Sciences, National Institute of Science Education and Research, HBNI, Jatni, Odisha 752050, India

^b School of Chemical Sciences, National Institute of Science Education and Research, HBNI, Jatni, Odisha 752050, India

^c Homi Bhabha National Institute, Training School Complex, Anushakti Nagar, Mumbai 400094, India

^d Hasselt University, Institute for Materials Research (IMO), Nano-Biophysics and Soft Matter Interfaces (NSI), Wetenschapspark 1, 3590 Diepenbeek, Belgium

^e IMEC, associated lab IMOMECE, Wetenschapspark 1, 3590 Diepenbeek, Belgium

* Corresponding Author

Equal Contribution

*** Corresponding author:**

Dr. V Badireenath Konkimalla

School of Biological Sciences,

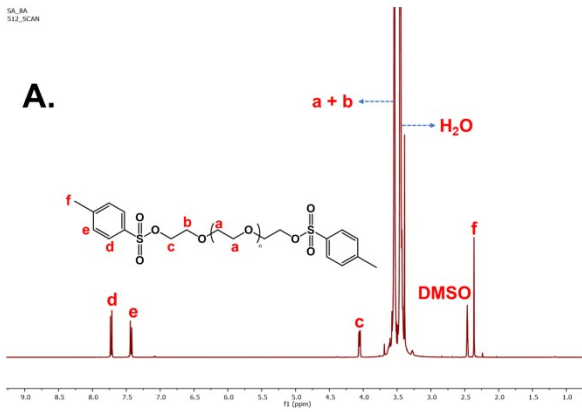
National Institute of Science Education & Research (NISER), PO- Bhipur-Padanpur, Via-
Jatni, District: - Khurda, Bhubaneswar, Orissa - 752 050, INDIA

E-mail: badireenath@niser.ac.in (V.B. Konkimalla)

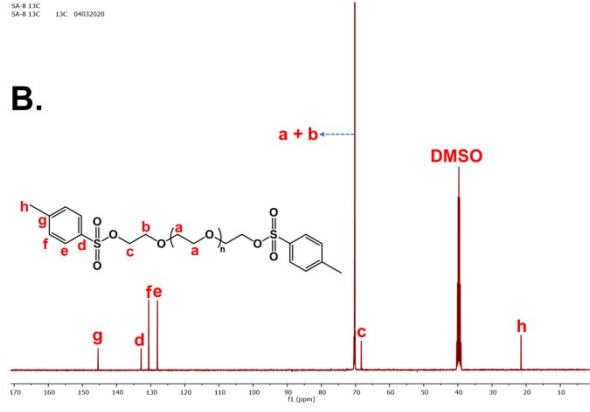
Tel: +91-674-249 42 11

SA-8A
312_SCAN

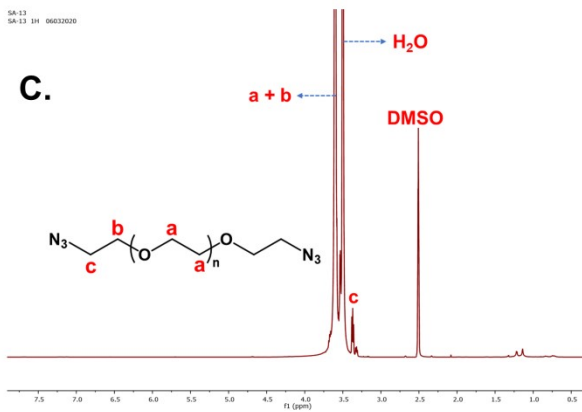
A.



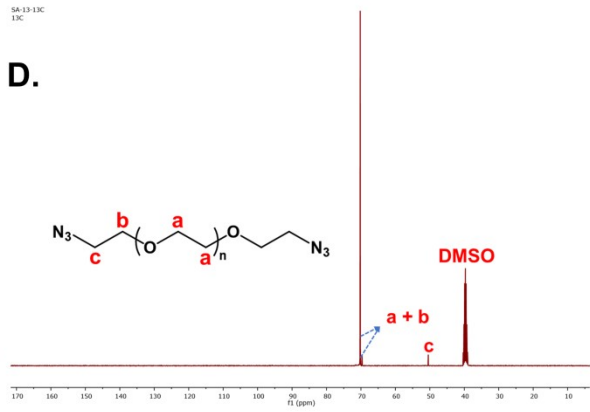
B.



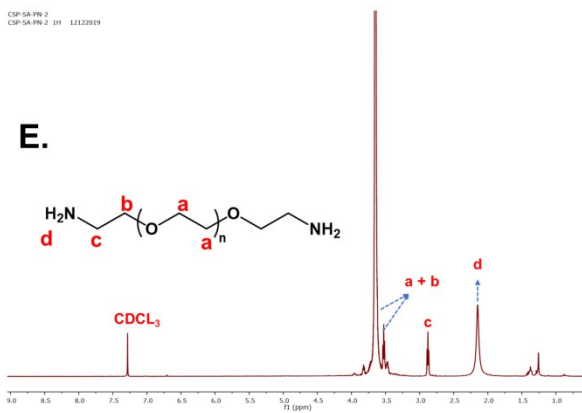
C.



D.



E.



F.

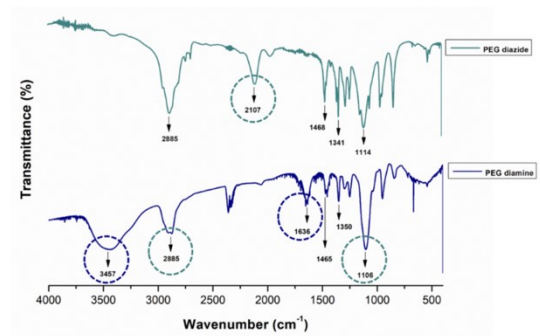
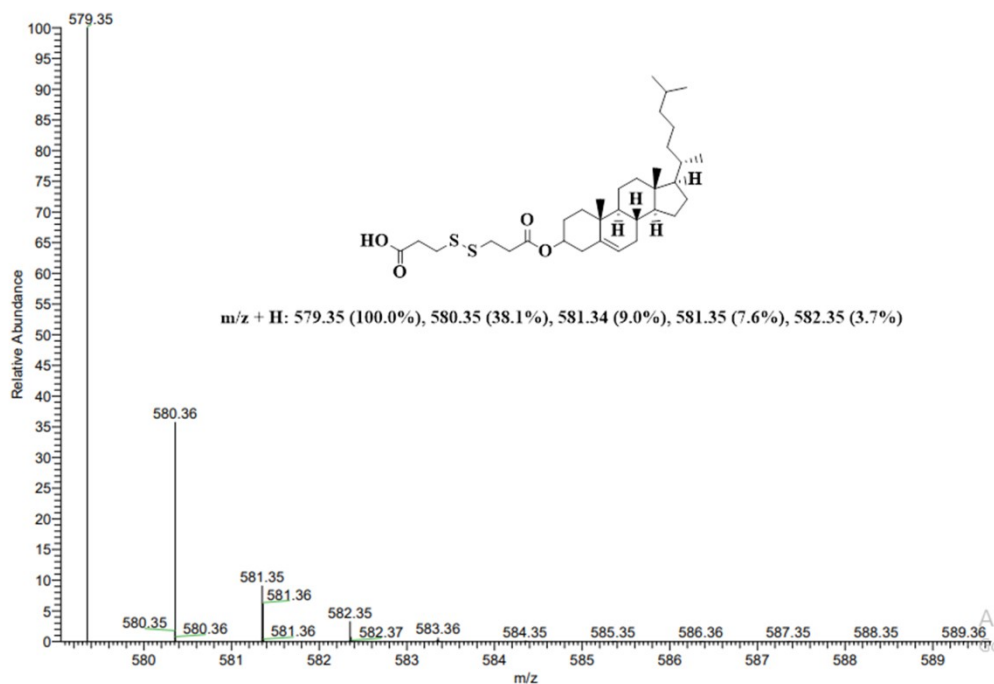


Fig. S1. ^1H NMR and ^{13}C NMR spectrum of tosylated PEG (A and B), PEG diazide (C and D), and ^1H NMR (E), and FTIR spectrum of PEG diamine (F)

A.

C33H54O4S2 +H: C33 H55 O4 S2 pa Chrg 1



B.

T: FTMS + p ESI Full ms [1500.0000-2500.0000]

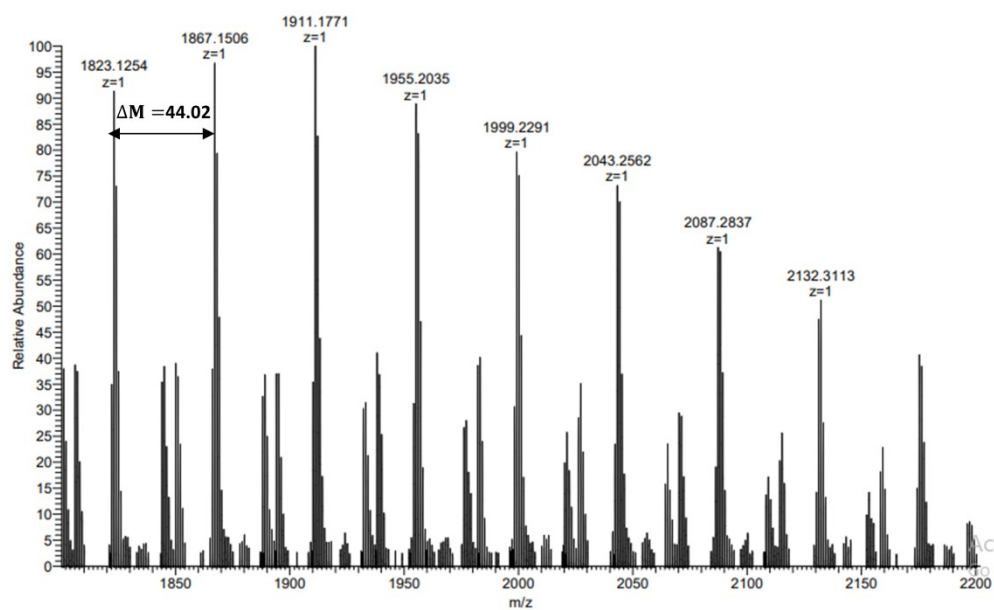


Fig. S2. Mass spectrum of Cholesterol-Dithiodipropionate (A) and PEG Diamine (B)

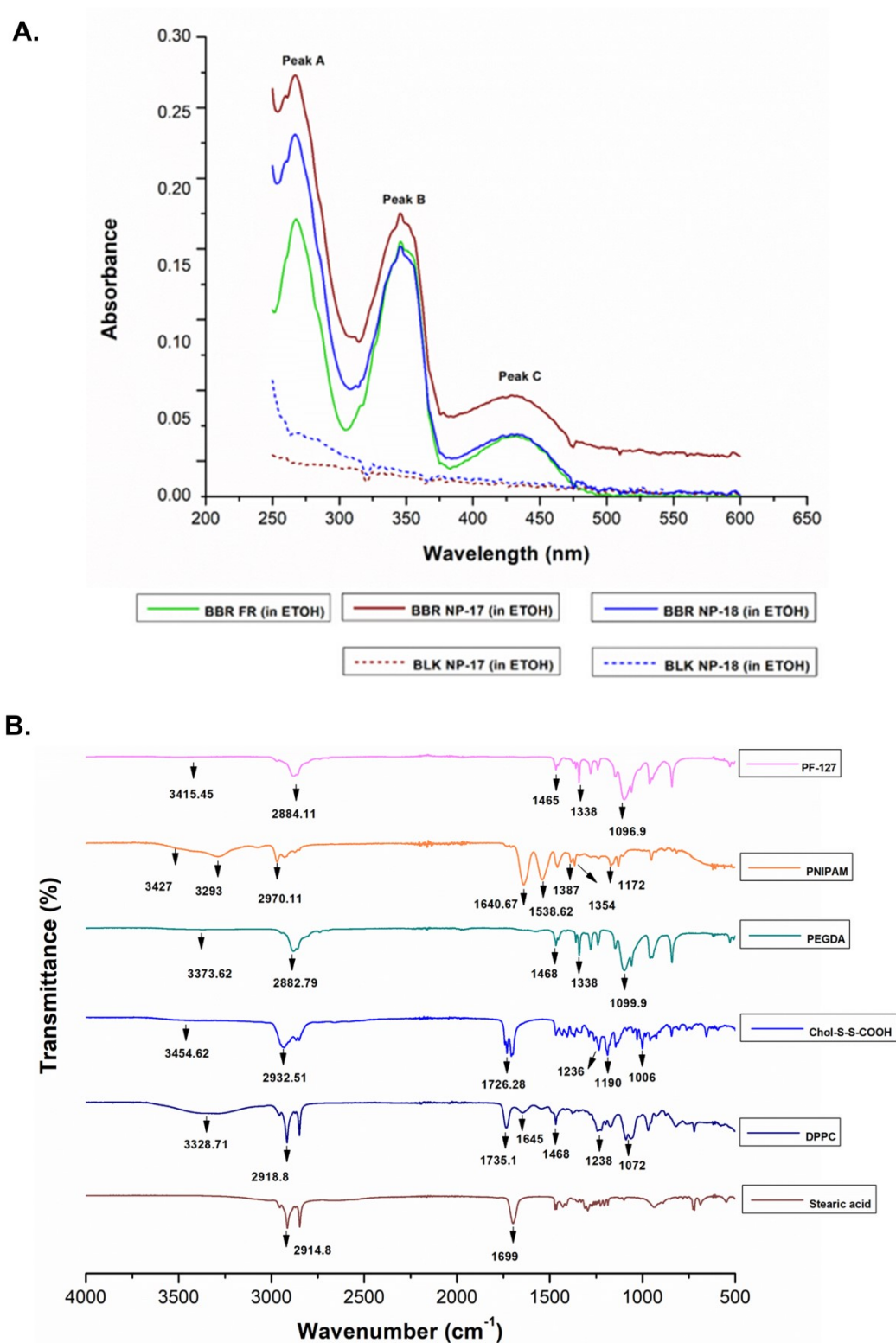


Fig. S3. Confirmatory study for the detection of BBR in BBR-loaded RS-PLHNCs by UV-Visible spectroscopy (A). FTIR spectra of free polymers and excipients i.e. PF-127, PNIPAM, PEGDA, disulfide cholesterol, DPPC, and stearic acid (B).

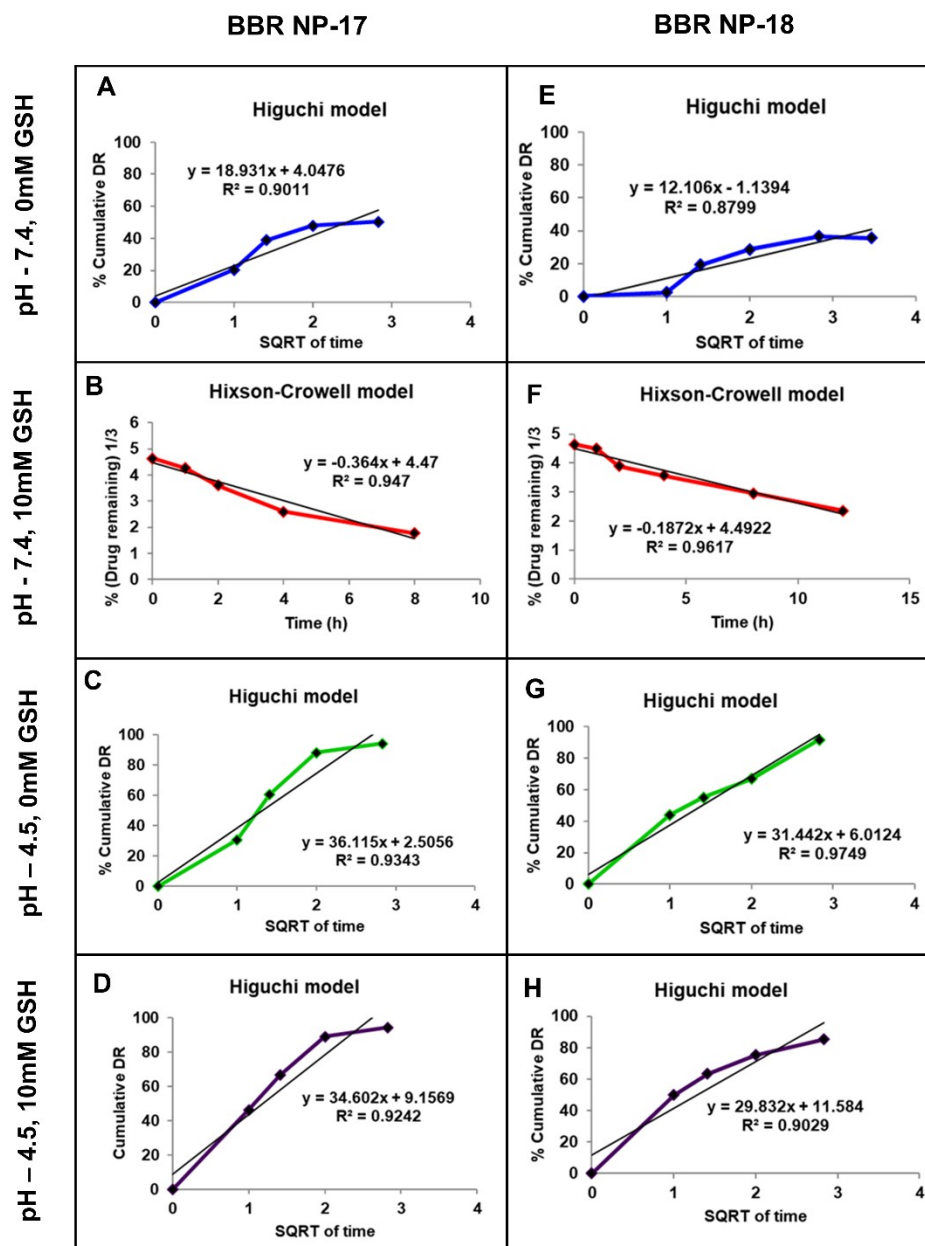


Fig. S4. Graphical illustration of the release kinetics of BBR from the nanocarrier system following a particular model (BBR NP-17 (A-D) and BBR NP-18 (E-H))

Table S1. Kinetic models of dissolution release profile of Berberine from the RS-PLHNCs (n=3)

(* denotes the best R² value of nanocarriers following a particular model)

Models	BBR NP-17				BBR NP-18			
	pH 7.4	pH 7.4 + 10mM GSH	pH 4.5	pH 4.5 + 10mM GSH	pH 7.4	pH 7.4 + 10mM GSH	pH 4.5	pH 4.5 + 10mM GSH
Zero order	0.675	0.827	0.760	0.688	0.750	0.868	0.799	0.643
First order	0.430	0.507	0.453	0.393	0.566	0.543	0.416	0.370
Higuchi	0.901*	0.944*	0.934*	0.924*	0.879*	0.953*	0.974*	0.902*
Hixson-Crowell	0.708	0.947*	0.887	0.859	0.769	0.961*	0.951*	0.805
Korsmeyer Peppas	0.449	0.539	0.472	0.393	0.759	0.672	0.401	0.361

Stability studies (upto 180 days)

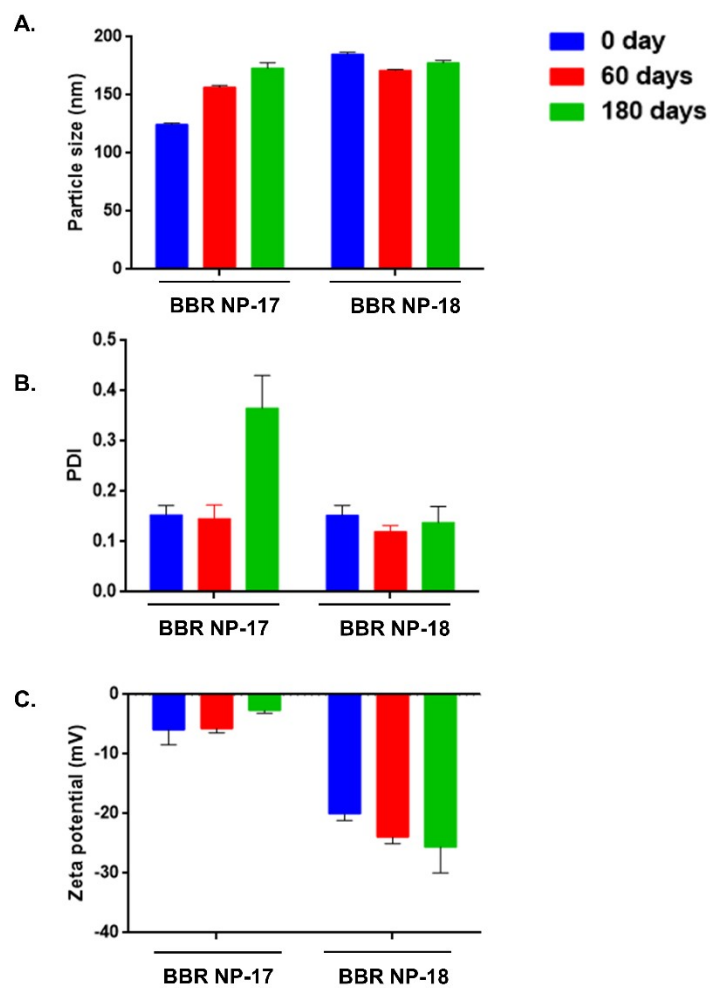
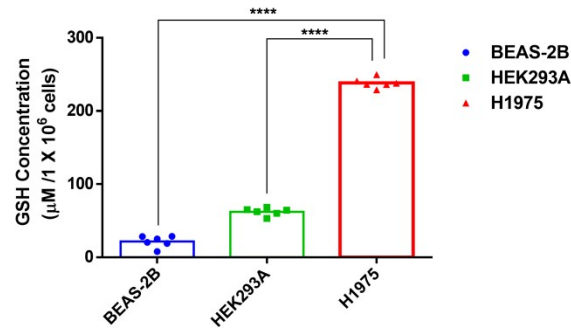


Fig. S5. Stability studies of BBR-loaded RS-PLHNCs (BBR NP-17 and 18) for 180 days at 4°C. Representative graph illustrates the changes in particle size (A), PDI (B), and zeta potential (C) occurred during the storage period.

A.



B.

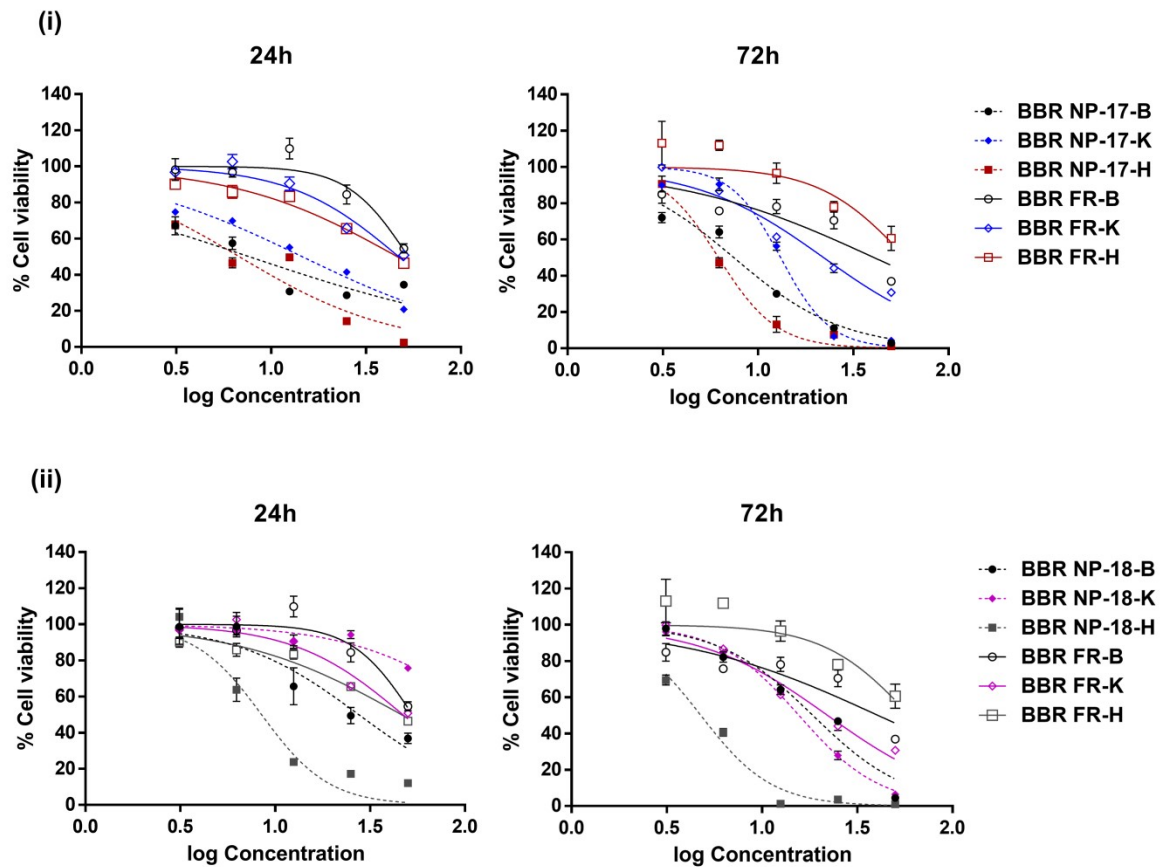


Fig. S6. Quantitative analysis of intracellular GSH levels in BEAS-2B, HEK293A, and H1975 cells (A). All the values are expressed in mean \pm SEM (n=6). A one way ANOVA multiple comparison test was used to compare the intracellular GSH level difference between normal cells (BEAS-2B & HEK293A cells), and cancer cells (H1975 cells).

Half maximal inhibitory graphs after the incubation of BBR NP-17 (B (i)) and BBR NP-18 (B (ii)) for 24 and 72 h in BEAS-2B, HEK293A and H1975 cells.

Abbreviations:

H: H1975 (lung cancer cell line). **BBR NP-17-H:** H1975 cells treated with BBR NP-17 nanocarriers, **BBR NP-18-H:** H1975 cells treated with BBR NP-18 nanocarriers, **BBR FR-H:** refers to H1975 cells treated with free form of BBR.

B: BEAS-2B (normal lung epithelial cells). **BBR NP-17-B:** BEAS-2B cells treated with BBR NP-17 nanocarriers, **BBR NP-18-B:** BEAS-2B cells treated with BBR NP-18 nanocarriers. **BBR FR-B:** refers to BEAS-2B cells treated with free form of BBR.

K: HEK293A (normal human embryonic kidney cells). **BBR NP-17-K:** HEK293A cells treated with BBR NP-17 nanocarriers, **BBR NP-18-K:** HEK293A cells treated with BBR NP-18 nanocarriers. **BBR FR-K:** refers to HEK293A cells treated with free form of BBR.

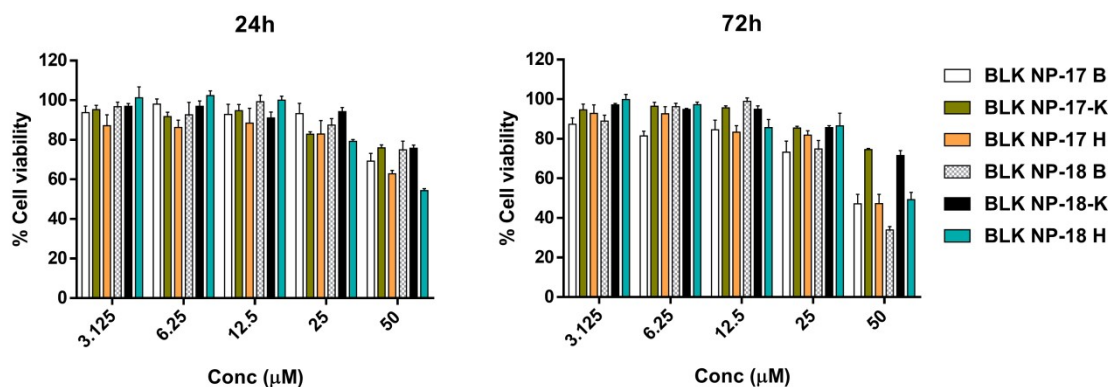


Fig. S7. Biocompatibility studies of BLK NP-17 and 18 in BEAS-2B, HEK293A, and H1975 cells. (data represented as mean \pm SEM, n=5). Difference in p values *p<0.05, **p< 0.01, ***p<0.001, and ****p<0.0001 was considered to be statistically significant and ns-non significant.

Abbreviations: B- BEAS-2B cells. **BLK NP-17-B-** BEAS-2B cells treated with BLK NP-17 nanocarriers, **BLK NP-18-B-** BEAS-2B cells treated with BLK NP-18 nanocarriers.

K- HEK293A cells. **BLK NP-17-K-** HEK293A cells treated with BLK NP-17 nanocarriers, **BLK NP-18-K-** HEK293A cells treated with BLK NP-18 nanocarriers.

H - H1975 cancer cells. **BLK NP-17-H-** H1975 cells treated with BLK NP-17 nanocarriers, **BLK NP-18-H-** H1975 cells treated with BLK NP-18 nanocarriers.

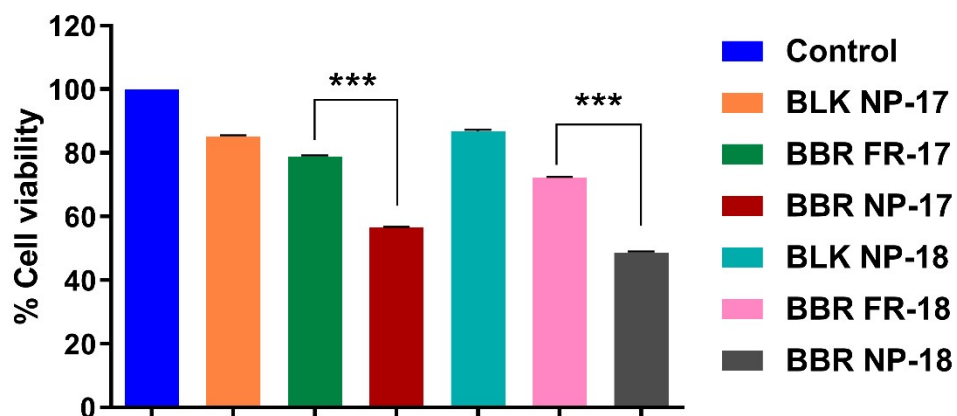


Fig. S8. Determination of cell viability (%) by cell counting method after the incubation of H1975 cancer cells with BLK NP-17 and 18, free BBR, BBR NP-17 and 18 for 24h. A one-way ANOVA test was used to evaluate the difference in cell viability between the groups treated with free BBR and BBR-loaded RS-PLHNCs. Statistical significance: * $p < 0.05$, ** $p < 0.01$, *** $p < 0.001$ and ns- non significant.

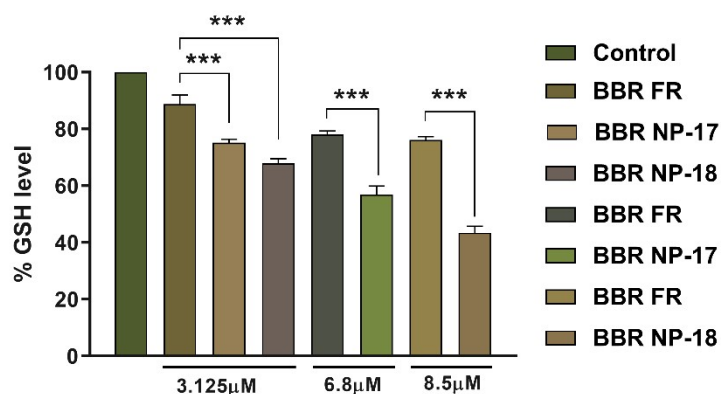
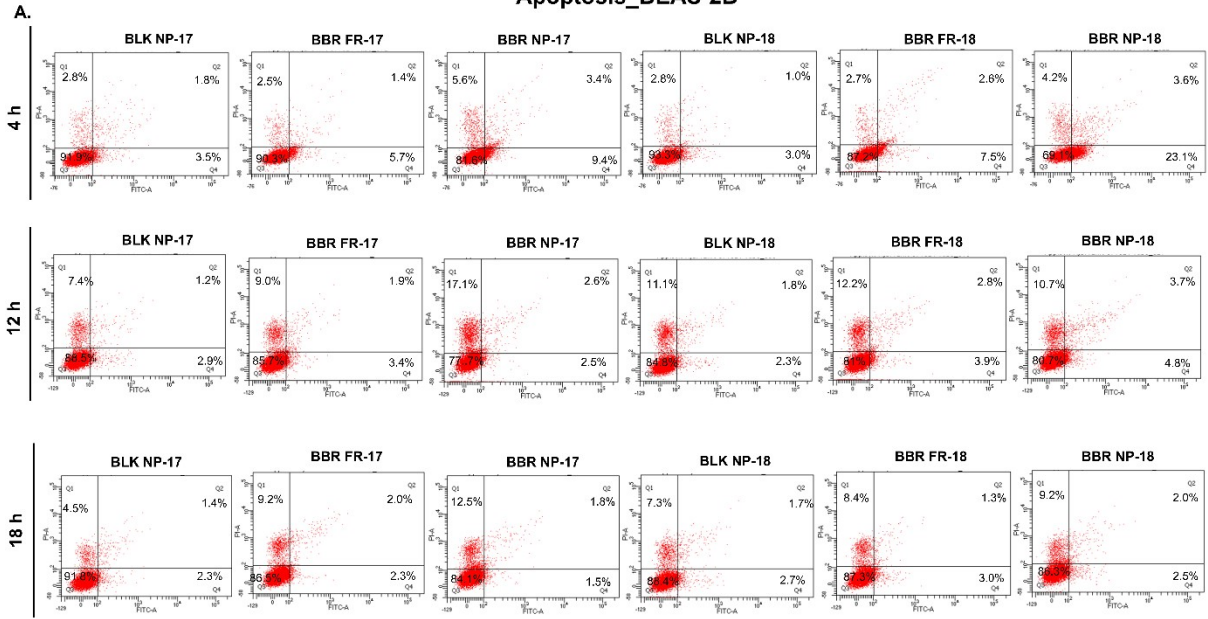
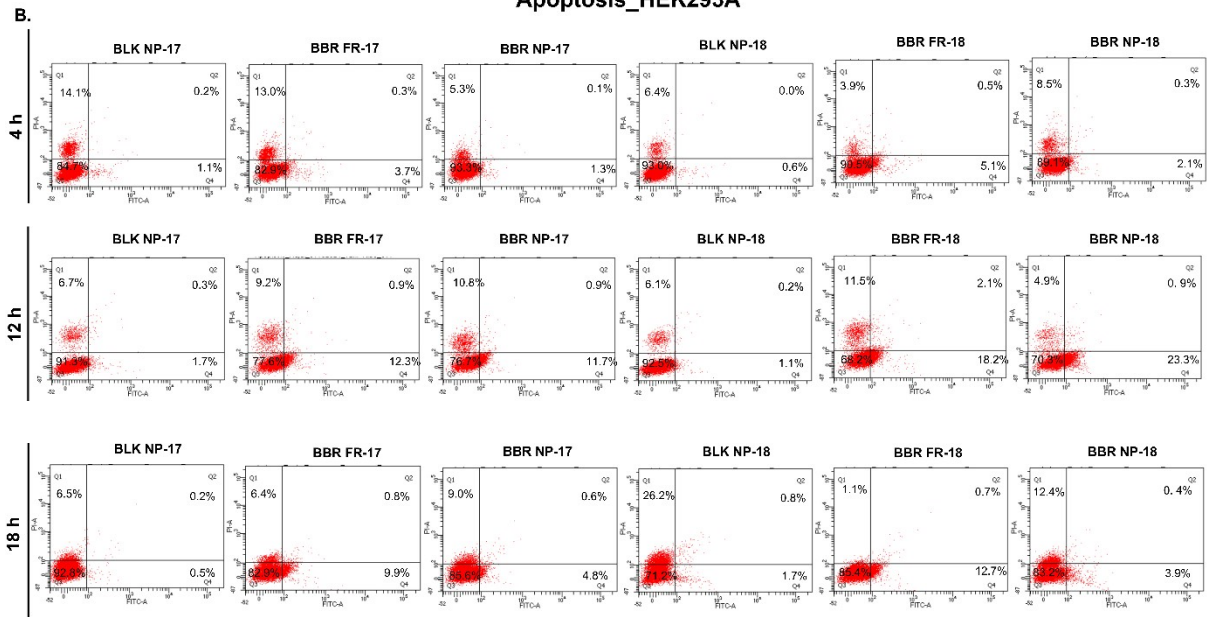


Fig. S9. Quantitative analysis of intracellular GSH levels in H1975 cancer cells after treatment with different concentrations of free BBR, BBR NP-17 and 18. All the values are expressed in mean \pm SEM (n=6). A one-way ANOVA test was employed to assess the differences in the decreased levels of intracellular GSH after treatment with free BBR and nanoparticulate form of BBR. Difference in p values *p<0.05, **p< 0.01, ***p<0.001, and ****p<0.0001 was considered to be statistically significant and ns-non significant

Apoptosis_BEAS-2B



Apoptosis_HEK293A



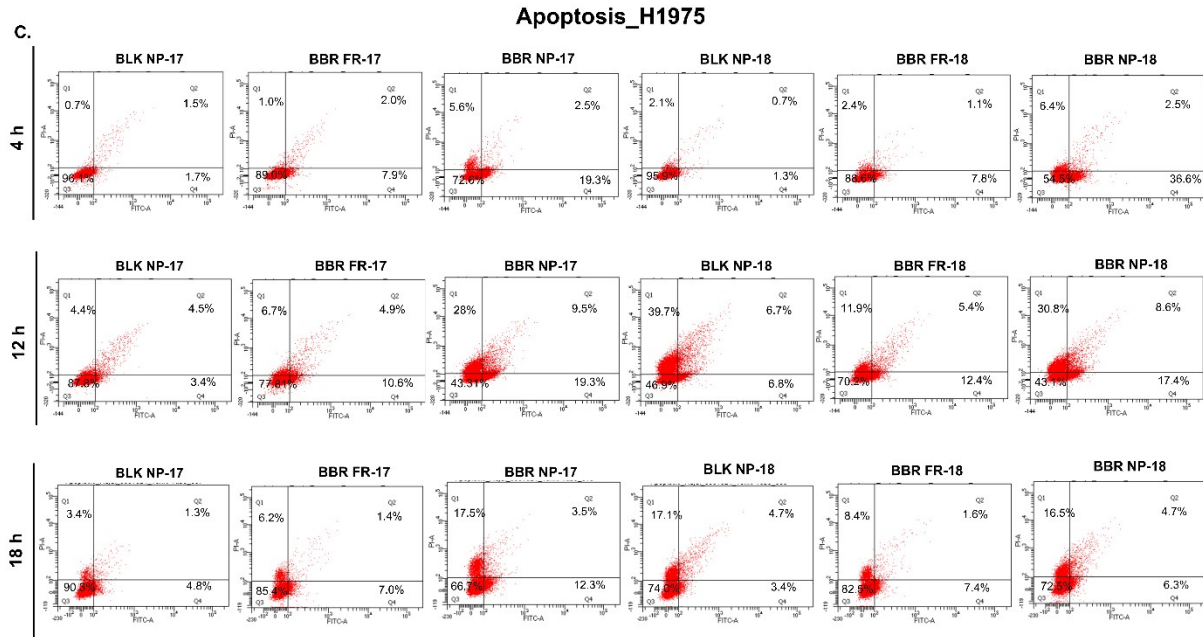


Fig. S10. Representative dot plots of % cell apoptosis from flow cytometry analysis. Q1 (Annexin V-FITC-/PI+) indicates necrosis, Q3 (Annexin V-FITC-/PI-) normal live cell population whereas, Q2 (Annexin V-FITC+/PI+) and Q4 (Annexin V-FITC+/PI-) represents late and early apoptosis respectively.

Table S2 Sequences of the primers used for real-time PCR (FP: Forward Primer RP: Reverse Primer)

Sl. No.	Gene	Primer sequence (5'- 3')		Tm (°C)	Amplicon size (bp)
1.	NOXA	FP	GTGCCAGCAGACCTGAAGG	60.67	151
		RP	CCTGGGAGGTCCCTTCTTG	59.01	
2.	PUMA	FP	GAGCAGCACCTGGAGTCG	60.13	180
		RP	CTGCTCCTCTTGTCTCCGC	60.15	
3.	MCL-1	FP	AGATGGCGTAACAAACTGGGG	60.61	188
		RP	ACTCCACAAACCCATCCCAGC	62.63	
4.	NQO1	FP	AGAAACGACATCACAGGGGAG	59.72	174
		RP	GGGCACCCCAAACCAATACA	60.54	
5.	TXRND1	FP	TCGACCCTTCTTGCTTTGGAT	59.65	103
		RP	AAGGAGGATGAAAACACCGGC	60.89	
6.	HMOX1	FP	GAGCTGCACCGAAGGGCT	62.40	169
		RP	GGTAGCGGGTATATGCGTGG	60.39	
7.	NFE2L2	FP	TCAGCTACTCCCAGGTTGC	59.02	135
		RP	GGGCAAGCGACTGAAATGTA	58.55	
8.	GAPDH	FP	ACCATCTTCCAGGAGCGAGA	60.32	147
		RP	GGCGGAGATGATGACCCTT	59.17	